AD-A118 232 AEROSPACE CORP EL SEGUNDO CA SPACE SCIENCES LAB F/G 22/2
DESCRIPTION OF P78-2 (SCATHA) SATELLITE AND EXPERIMENTS.(U)
JUL 82 J F FENNELL F04701-81-C-0082
UNCLASSIFIED TR-0082(2940-05)-10 SD-TR-82-43 NL

1 OF 1
AD
A118232

END
DATE
FILMED
9-82
DTIC

REPORT SD-TR-82-43

AD A118232

Description of P78-2 (SCATHA) Satellite and Experiments

J. F. FENNELL
Space Sciences Laboratory
Laboratory Operations
The Aerospace Corporation
El Segundo, Calif. 90245

12 July 1982

APPROVED FOR PUBLIC RELEASE;
DISTRIBUTION UNLIMITED

Prepared for

SPACE DIVISION
AIR FORCE SYSTEMS COMMAND
Los Angeles Air Force Station
P.O. Box 92960, Worldway Postal Center
Los Angeles, Calif. 90009

This report was submitted by The Aerospace Corporation, El Segundo, CA 90245, under Contract No. F04701-81-C-0082 with the Space Division, Deputy for Technology, P.O. Box 92960, Worldway Postal Center, Los Angeles, CA 90009. It was reviewed and approved for The Aerospace Corporation by H. R. Rugge, Director, Space Sciences Laboratories. Major George A. Kuck, SD/YLS, was the project officer for the Mission-Oriented Investigation and Experimentation (MOIE) Program.

This report has been reviewed by the Public Affairs Office (PAS) and is releasable to the National Technical Information Service (NTIS). At NTIS, it will be available to the general public, including foreign nations.

This technical report has been reviewed and is approved for publication. Publication of this report does not constitute Air Force approval of the report's findings or conclusions. It is published only for the exchange and stimulation of ideas.

George A. Kuck

George A. Kuck, Major, USAF
Project Officer

Jimmie H. Butler

Jimmie H. Butler, Colonel, USAF
Director of Space Systems Planning

FOR THE COMMANDER

Norman W. Lee

Norman W. Lee, Jr., Col, USAF
Deputy for Technology

UNCLASSIFIED

SECURITY CLASSIFICATION OF THIS PAGE (When Data Entered)

REPORT DOCUMENTATION PAGE

READ INSTRUCTIONS BEFORE COMPLETING FORM

1. REPORT NUMBER SD-TR-82-43	2. GOVT ACCESSION NO. AD-A118232	3. RECIPIENT'S CATALOG NUMBER
4. TITLE (and Subtitle) DESCRIPTION OF P78-2 (SCATHA) SATELLITE AND EXPERIMENTS		5. TYPE OF REPORT & PERIOD COVERED
		6. PERFORMING ORG. REPORT NUMBER TR-0082(2940-05)-10
7. AUTHOR(s) Joseph F. Fennell		8. CONTRACT OR GRANT NUMBER(s) F04701-81-C-0082
9. PERFORMING ORGANIZATION NAME AND ADDRESS The Aerospace Corporation El Segundo, Calif. 90245		10. PROGRAM ELEMENT, PROJECT, TASK AREA & WORK UNIT NUMBERS
11. CONTROLLING OFFICE NAME AND ADDRESS Space Division Air Force Systems Command Los Angeles, Calif. 90009		12. REPORT DATE 12 July 1982
		13. NUMBER OF PAGES 34
14. MONITORING AGENCY NAME & ADDRESS(if different from Controlling Office)		15. SECURITY CLASS. (of this report) Unclassified
		15a. DECLASSIFICATION/DOWNGRADING SCHEDULE

16. DISTRIBUTION STATEMENT (of this Report)

Approved for public release; distribution unlimited

17. DISTRIBUTION STATEMENT (of the abstract entered in Block 20, if different from Report)

18. SUPPLEMENTARY NOTES

19. KEY WORDS (Continue on reverse side if necessary and identify by block number)

SCATHA satellite
Space experiments
Spacecraft charging
Space environment

20. ABSTRACT (Continue on reverse side if necessary and identify by block number)

The P78-2 (SCATHA) satellite was placed into a near synchronous orbit in early February 1979. The satellite was a part of a joint U. S. Air Force/NASA program to study spacecraft charging. The satellite has its spin axis approximately parallel to the earth's equatorial plane. This allows good pitch angle coverage by the particle experiments. The experiment complement consists of a complete set of plasma, energetic particle, composition, field and wave experiments. The satellite has already provided over two years of data; about

DD FORM 1473 (FACSIMILE)

UNCLASSIFIED

SECURITY CLASSIFICATION OF THIS PAGE (When Data Entered)

19. KEY WORDS (Continued)

20. ABSTRACT (Continued)

one year (February, 1979 to March, 1980) of it has been provided to the experimenters as formatted digital tapes. The data is of very high quality and the coverage is good (> 90%).

CONTENTS

FIGURES

TABLES

Introduction

The P78-2 satellite, almost universally called the SCATHA (Spacecraft Charging AT High Altitude) satellite, was conceived as the flight test portion of a joint U. S. Air Force/NASA spacecraft charging program. A detailed description of the program and the P78-2 spacecraft can be found in a report by Stevens and Vampola (1978). The objectives of the satellite flight were twofold; one was to obtain environmental and engineering information so as to provide design criteria, materials, techniques, tests and analytical methods to ensure control of the charging of satellite surfaces. The second objective was to collect scientific data of interest to each experiment sponsor and the scientific community. Key areas of scientific investigation include understanding plasma-wave interactions, substorm studies and further studies of the energetic ring current.

Satellite Parameters

The satellite was launched on 30 January 1979 and inserted into its final orbit on 2 February 1979. The orbit of P78-2 was chosen to cover the near synchronous region close to the geographic equator. The apogee and perigee are ~ 43200 km ($R \sim 7.8$ Re) and 27500 km ($R \sim 5.3$ Re) respectively. The inclination of the orbit is ~ 7.8° with apogee and perigee lying in the earth's equatorial plane. The orbital period is ~ 23.6 hrs and thus the mean position of the satellite drifts eastward in longitude at ~ 5.3° per day (see Figure 1). On 5 February apogee was at ~ 190° east longitude and 9.3 hrs MLT.

The satellite is spin stabilized (spin rate ~ 1 rpm) with the spin axis in the orbit plane and maintained approximately perpendicular to the satellite-sun line. This allows those experiments with view axes approximately perpendicular to the spin axis to scan a large range of angles relative to the magnetic field. It also allows those sensors on the end of the satellite with fields of view parallel to the spin axis to be viewing nominally perpendicular to $\underline{B}$. The experiment positions are shown in Figure 2.

The satellite is cylindrical and about 1.75 m in length and diameter. Seven experiment booms are deployed on orbit. These are also shown in Figure 2. Most of the cylinder is covered with solar cells. Provisions were made for providing conductive surfaces around the particle experiment apertures. For details of the surface materials see Stevens and Vampola (1978).

The SC1 experiment (see Experiment Section) measures VLF and HF signals. To maintain low noise signature in the frequency ranges of interest the experiment and vehicle systems section was designed as a Faraday cage. External equipment was housed in shielded enclosures and subject to stringent electromagnetic control. All external lines were doubly shielded and the power system source impedance was held to < 20 mohms from DC to 10 MHz. For magnetic cleanliness a zero-net-current cabling approach was used and the solar arrays were back-wired to cancel fields generated by array currents. The result was an electromagnetically and magnetically clean satellite as is evidenced by the high quality of the wave and magnetometer data.

Two tape recorders are used to provide nearly complete coverage in every orbit. Each has a 12-hour capacity at the 8192 bps basic data rate. There is also a direct FM channel which provides frequency response up to 5 kHz. It is used in a number of different modes by the VLF wave, magnetometer, DC electric field, and two plasma experiments. From 5 February to the present the satellite has averaged > 90% coverage for the digital data (see Figure 3 for first year of coverage). The FM data is limited to ~ 2 hrs per day by ground station resources. The primary

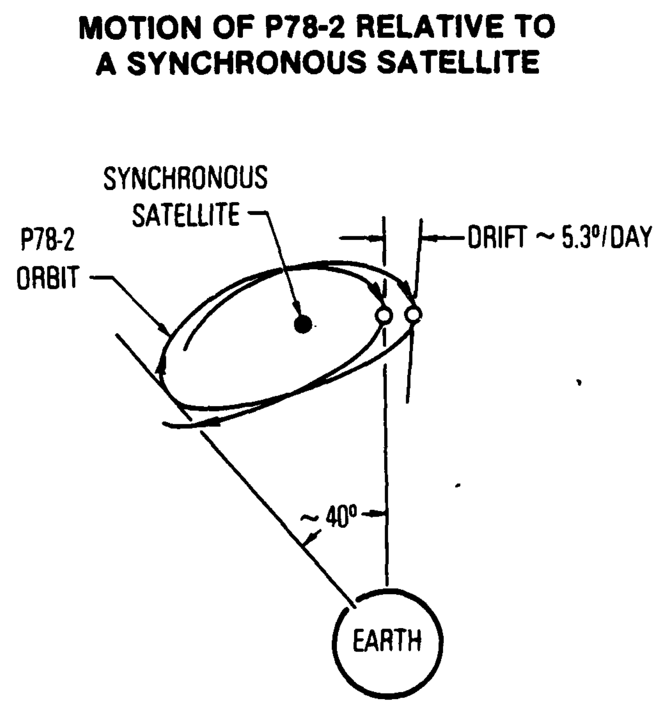

Fig. 1. Diagram showing the orbit of P78-2 relative to a synchronous satellite. The distance between the circle points represents the daily longitudinal drift.

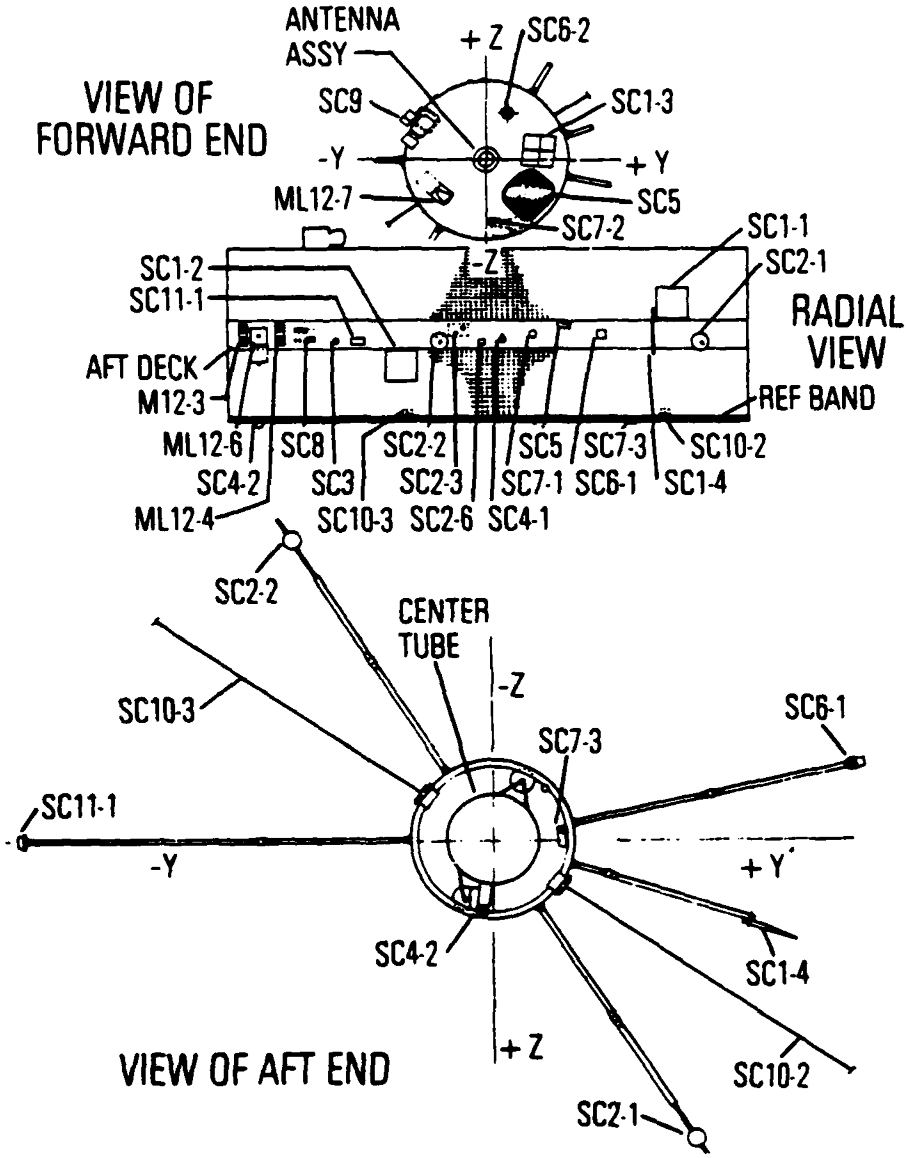

Fig. 2. Experiment and boom locations on the satellite (from Stevens and Vampola, 1978)

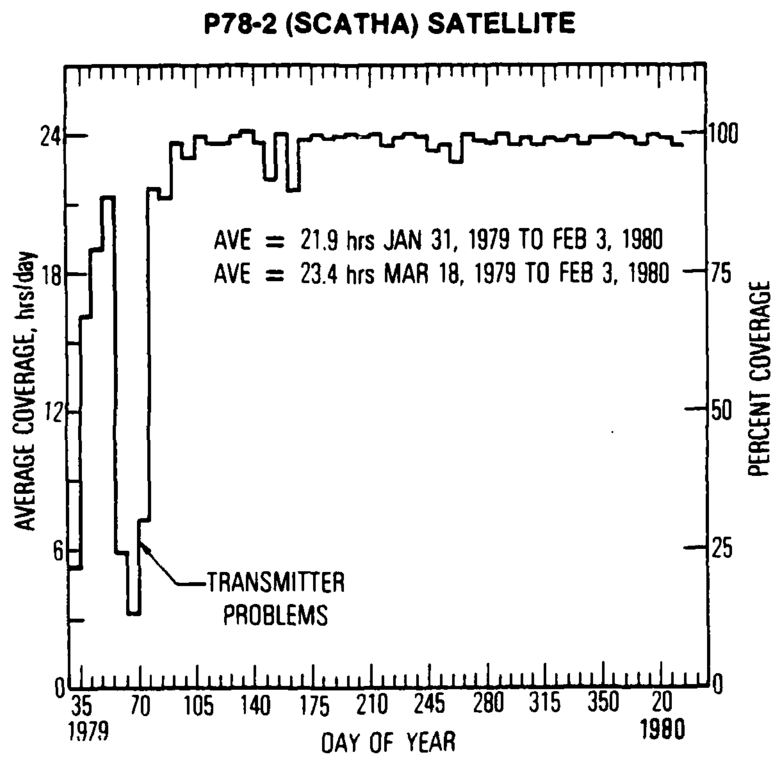

Fig. 3. Data coverage for the first year of operations

period of data lapse was from 17 February to 16 March 1979 when transmitter problems were experienced.

Experiments

Table 1 shows the experiment identifiers and the principal investigators. The individual experiment components are further detailed in Table 2 with the date of first operation. Table 3 shows the particle detector characteristics. The operation of the ion and electron beam systems (SC4-2 and SC4-1) are constrained and usually occur during the eclipse seasons. Each beam system operation has a duration from a few minutes to ~ 1 hr. Many of the plasma experiments are turned off during the electron beam operations because of the high beam currents which can be emitted (1 μA to 12 mA).

Two of the experiments, SC6 and SC7, failed shortly after being turned on. SC7 collected ~ 10 days of data (see Table 2). These failures mean there isn't a direct plasma density measurement for most of the mission. Some attempts are being made to use the plasma analyzers (especially SC9) plus the VLF wave data to estimate the plasma density.

SC1 Engineering and Wave Experiments

As Table 2 shows, the SC1 experiment contains both science and engineering instruments. The engineering experiments consist of satellite surface potential monitors (SSPMs) and a transient pulse shape analyzer (TPSA). The SSPMs measure the potential of selected materials such as Kapton, Teflon, etc. and the bulk current through these samples. These provide information about the response (charging) of such materials in the near synchronous plasma environment.

The TPSA measures the shape of electromagnetic pulses in the time domain from 7 nsec to 3.7 msec. The objective is to verify that electrical discharges are occurring on the satellite and to correlate the occurrence with the other data. The pulses are measured on four sensors, three internal and one external to the Faraday cage. For details of this and the SSPM experiment refer to the report by Stevens and Vampola (1978) and those by Mizera and Koons (see reference list).

The primary SC1 science experiment is the VLF wave experiment (Koons, 1981; Stevens and Vampola, 1978). The experiment employs two antennas, an air-core loop and the 100 m tip-to-tip

Table 1. P78-2 (SCATHA) Experiments

Experiment Identification	Title	Principal Investigator
SC1	Engineering Experiments Plus VLF and HF Receivers	H. C. Koons The Aerospace Corporation
SC2	Spacecraft Sheath Fields Plus Energetic Ions	J. F. Fennell The Aerospace Corporation
SC3	High Energy Particle Spectrometer	J. B. Reagan Lockheed Palo Alto Research Lab
SC4	Satellite Electron and Positive Ion Beam System	H. A. Cohen Air Force Geophysics Lab
SC5	Rapid Scan Particle Detector	D. Hardy Air Force Geophysics Lab
SC6	Thermal Plasma Analyzer	R. C. Sagalyn Air Force Geophysics Lab
SC7	Light Ion Mass Spectrometer	D. L. Reasoner NASA Marshall Space Flight Center
SC8	Energetic Ion Composition Experiment	R. G. Johnson Lockheed Palo Alto Research Lab
SC9	UCSD Charged Particle Experiment	S. E. Deforest E. C. Whipple Univ. of Calif. at San Diego
SC10	Electric Field Detector	T. L. Aggson NASA Goddard Space Flight Center
SC11	Magnetic Field Monitor	B. G. Ledley NASA Goddard Space Flight Center
ML12	Spacecraft Contamination Plus Thermal Control Materials Monitoring	D. F. Hall The Aerospace Corporation
TPM	Transient Pulse Monitor	R. Adamo SRI International

Table 2. Measurements Made by Experiments

Experiment Identification	Parameters Measured	Comments
SC1	(1) Surface potentials of various materials	Turned on 5 Feb.
	(2) E&M VLF wave analyzer (~0 Hz to 300 kHz)	Turned on 8 Feb.
	(3) E&M RF wave analyzer (2 MHz to 30 MHz)	Turned on 8 Feb.
	(4) Transient pulse shape analyzer (Pulse time domain 7 ns to 3.7 ms; amplitude 3 mV to 1910 V)	Turned on 5 Feb.
SC2	(1) Potentials of spherical probes (common mode, $\pm$ 0.02 to $\pm$ 700 volts)	Turned on 8 Feb. Failed 30 March.
	(2) Low energy electrons and ions (15 eV/q to 18.6 keV/q)	Turned on 2 Feb.
	(3) Energetic protons (17 keV to > 3.3 MeV)	Turned on 31 Jan.
	(4) Energetic ions, $Z \geq 2$ (E_I > 90 keV/nucleon)	Turned on 31 Jan.
SC3	High energy electrons and protons (E_e = 50 keV to 5.3 MeV; E_p = 1.0 MeV to 200 MeV)	Turned on 31 Jan.
SC4	(1) Electron beam emission system (E_e = 50 eV to 3.0 keV; I_e = 1.0 μA to 13 mA)	Turned on 30 March. Pulse mode failed 30 March.
	(2) Positive ion (Xenon) beam emission system (E_I = 1.0 and 2.0 keV; I_I = 0.3 mA to 2.0 mA)	Turned on 11 Feb. Includes electron source for beam neutralization.
SC5	Electrons and ions (E_e = 50 eV to ~1.0 MeV; E_I = 50 eV to 35 MeV)	Turned on 9 Feb. Includes ESAs and particle telescopes.
SC6	Thermal electrons and ions (E_e and E_i from ~0 eV to 100 eV)	Failed during checkout.
SC7	Light ion density, temperature and composition (E_I = 0.0 to 100 eV; H^+, He^+, O^+)	Turned on 7 Feb. Failed on 17 Feb.
SC8	(1) Ion Composition of energetic plasma (E_I = 100 eV to 32 keV; M = 0.8 to 160 AMU with M/Q = 1, 2, 4 or 16)	Turned on 8 Feb.
	(2) Low energy electrons (E_e = 70 eV to 24 keV in 4 channels)	Turned on 8 Feb.
SC9	Electrons and ions (one set with E = few eV to 81 keV, two others with E = 0.2 eV to 1.55 keV)	Turned on 1 Feb. One low range ion sensor views ⊥ to spin axis. One low and one high range sensor have variable view directions.
SC10	DC and ELF electric fields and satellite potential (ELF 0.2 to 200 Hz; common mode voltage 0 to $\pm$ 5 keV)	Turned on 25 Feb. Booms fully extended on 9 March.
SC11	DC and ELF magnetic field (range from $\pm$ 0.3 to $\pm$ 500 nT; ELF ~1 to 100 Hz)	Turned on 22 Feb.
ML12	(1) Contaminant mass deposition rates	Turned on 30 Jan.
	(2) Solar absorptance of test materials	Turned on 30 Jan.
TPM	Electromagnetic pulse environment on satellite (Pulse amplitude 2 mV to 240 V, current 2 mA to 1700 A)	Turned on 8 Feb.

Table 3. Particle Detector Characteristics

Species/ Number	Energy Min-Max	ΔE/E	Δt (sec)	Geometrical Factors (cm^2-sr)	Comments
Electrons					
SC6	1-100 eV		0.1	~0.4	
SC9	0.2 eV-1.55 keV	0.2	0.25, 0.04, or 0.0005	1.6×10^{-4}	Programmable Resolution
SC5	0.05-1.7 keV	0.8	0.2	10^{-4}	
SC2	6 eV-18 keV	0.07	0.1	1.7×10^{-4}	
SC9	1 eV-81 keV	0.2	0.25, 0.04, or 0.0005	1.6×10^{-4}	Programmable Resolution
SC5	1.7-60 keV	0.8	0.2	10^{-4}	
SC5	30-550 keV	0.4 to 1.3	0.1 or 0.2	3.5×10^{-3}	
SC3	0.05-5.1 MeV	0.1 to 1	0.5	3×10^{-3}	Programmable Resolution
SC3	5.1-10.0 MeV	Integral	0.5	3×10^{-3}	Programmable Resolution
Protons					
SC9	0.2 eV-1.55 keV	0.2	0.25, 0.04, or 0.0005	3.2×10^{-4}	Programmable Resolution
SC5	0.05-1.7 keV	0.8	0.2	10^{-2}	
SC2	5 eV-14 keV	0.1	0.1	6.7×10^{-4}	
SC9	1 eV-81 keV	0.2	0.25, 0.04, or 0.0005	3.2×10^{-4}	Programmable Resolution
SC5	1.7-60 keV	0.8	0.2	10^{-2}	
SC5	70-725 keV	0.5	0.1 or 0.2	2×10^{-2}	
SC2	17->3300 keV		1.0	2×10^{-3}	
SC5	0.725-35 MeV	0.5 to 0.9	0.1 or 0.2	2×10^{-2}	
SC3	1-200 MeV	0.003 to 0.3	0.5	3×10^{-3}	Programmable Resolution
Ions					
SC6	1-100 eV		0.1	~0.4	
SC7	1-100 eV	0.2	0.06	2×10^{-3}	H^+, $^4He^+$, $^{16}O^+$
SC8	0.1-32 keV	0.05	32	10^{-3}	Δm/m is mass dependent 1 - 160 AMU
SC2	>90 keV/Nucleon	Integral	1.0 or 0.25	3.6×10^{-4}	
SC3	6-60 MeV	0.01 to 0.2	0.5	3×10^{-3}	Programmable Resolution

dipole from the SC10 experiment. The electric field receiver has a sensitivity of 5×10^{-7} $V/(mHz^{1/2})$ at 1.3 kHz and 10^{-7} $V/(mHz^{1/2})$ at 10.5 kHz. The magnetic loop is electrostatically shielded, has an effective area of 575 m^2 at 1.3 kHz, and is mounted on a two-meter boom. The sensitivity of the magnetic receiver is 3×10^{-6} $\gamma/Hz^{1/2}$ at 1.3 kHz and has a 60 dB dynamic range. There are eight narrow band filter (bandwidth ± 7.5%) outputs at 0.4, 1.3, 2.3, 3.0, 10.5, 30, 100 and 300 kHz and a broadband mode (0 to 5 kHz). The broadband data is taken for one to two hours per day. The filter data is taken continuously. Figure 4a shows an example of the broadband wave data for a period when both chorus and hiss are present. Figure 4b shows filter data averaged over a period including Figure 4a. The wave intensity is plotted as a function of the angle between the antennae axes and $\underline{B}$. Both the 400 Hz and 1.3 kHz data are from portions of the spectrum occupied by the hiss band. These data indicate $\underline{k}$ is nearly parallel to $\underline{B}$ (Koons, 1981).

SC2 Plasma and Energetic Ion Experiments

The SC2 experiment also has science and engineering applications. The spherical probes provide the potential between a floating sphere and the satellite frame (Stevens and Vampola, 1978; Fennell and Croley, 1981). A sample of this data is shown in Figure 8 and described, with SC4, below. As shown in Table 2 the probe voltage measuring circuitry failed on March 30, 1979. The electrostatic analyzers in the probes and on the spacecraft are identical and measure ions and electrons with energies from a few eV to ~ 18 keV (see Table 2), perpendicular to the spin axis. A complete twenty-one channel spectrum is formed in three seconds. This provides a good two dimensional distribution function in one spin period. An example of such electron and ion distribution functions are shown in Figure 5. These data show field aligned bouncing electrons and field-aligned ion beams. These have been described in a paper by Richardson et al. (1981) and occur primarily near local midnight during substorms.

SC2 also measures energetic ions with a temporal resolution of 250 msec for He and the CNO group and one sec for protons. An example of a He angular distribution is shown in Figure 6a (from Blake and Fennell, 1981). This shows that the angular distribution is flat for > 85°,

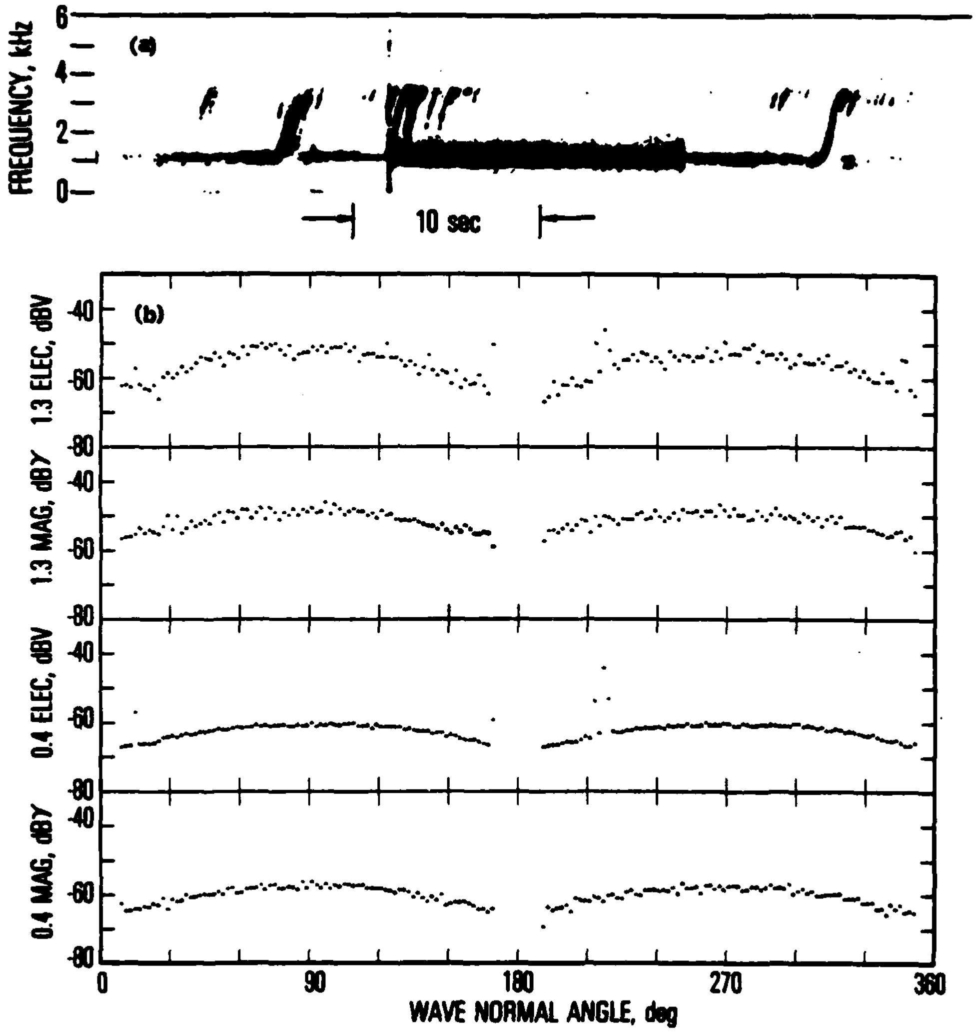

Fig. 4. (a) Chorus emissions emerging from hiss bands on 19 July 1979 at L = 6.01 and MLT = 15.4. (b) Wave amplitudes as a function of the angle between the antenna axis and the geomagnetic field direction. This period includes (a) above. Taken from Koons and Cohen, 1981.

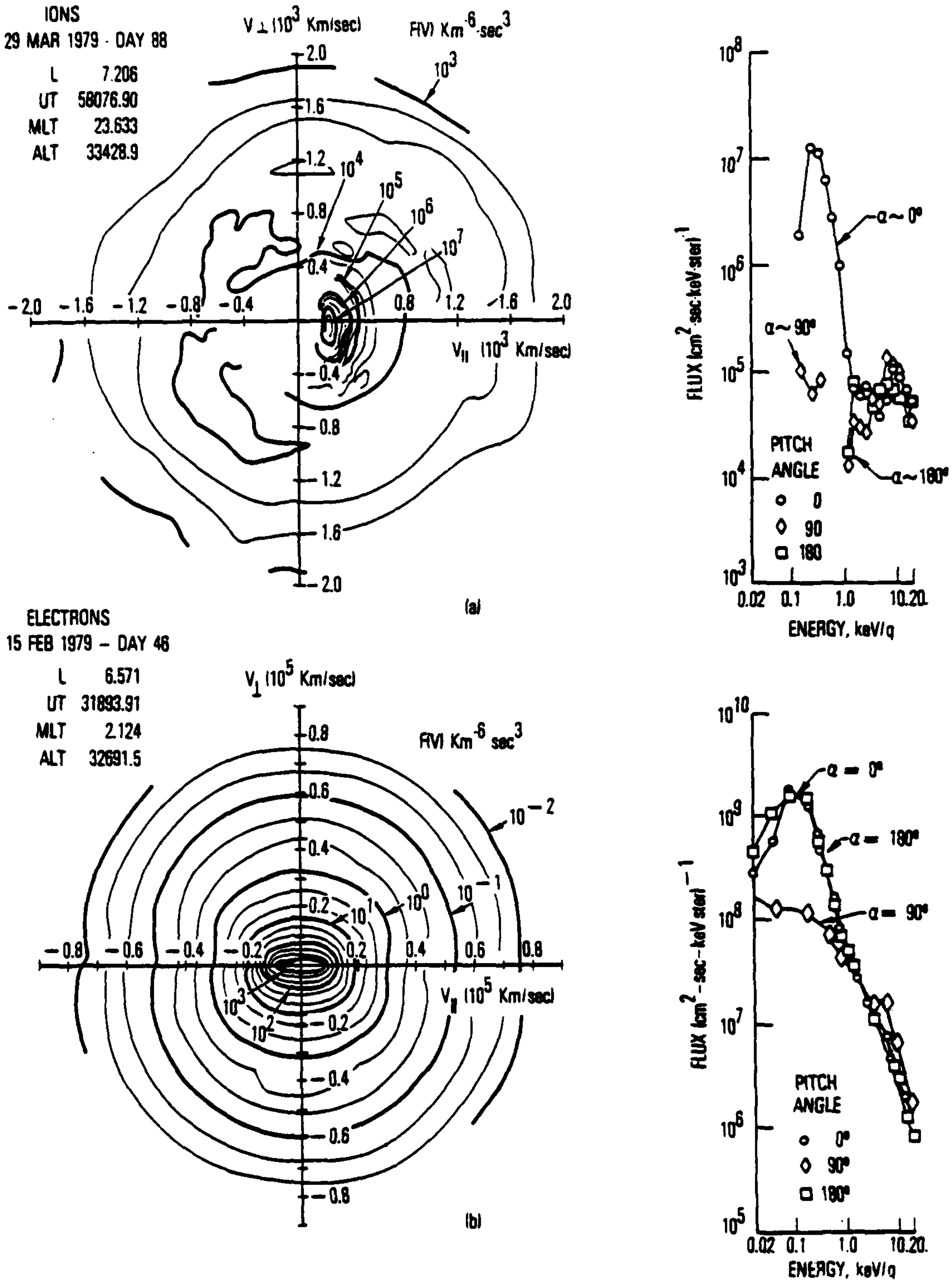

Fig. 5. (a) Ion velocity space distribution (left panel) and selected energy spectra (right panel) taken on 29 March 1979. (b) Electron velocity space distribution (left panel) and selected energy spectra (right panel) taken on 15 February 1979. These are from Richardson et al. (1981).

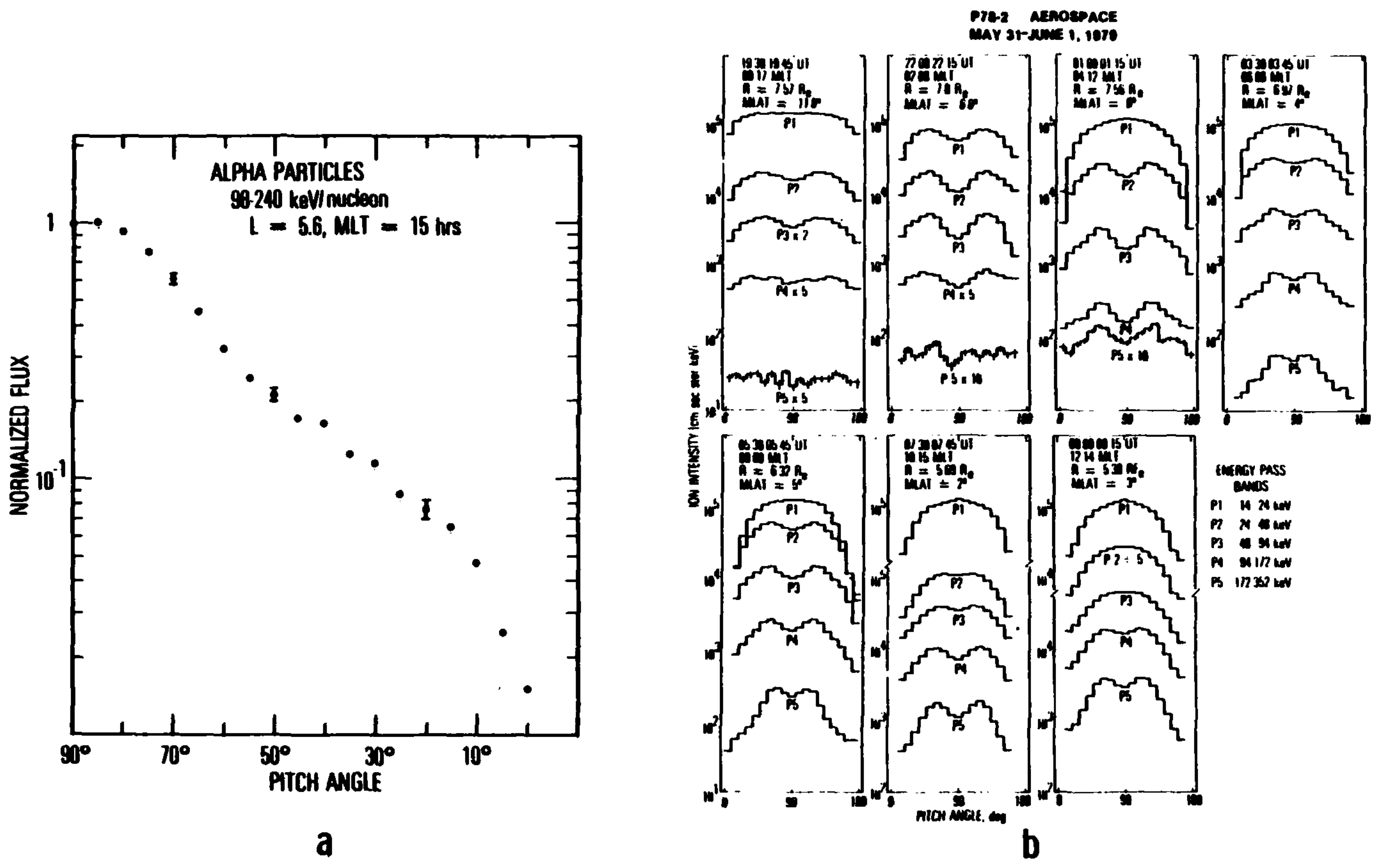

Fig. 6. (a) Alpha particle equatorial pitch angle distribution taken on 30 March 1979 with the Aerospace SC2 experiment. (b) Proton pitch angle distributions for several local times, L shells, and magnetic latitudes on 31 May and 1 June 1979 taken with the Aerospace SC2 experiment. (After Blake and Fennell, 1981).

falls rapidly until $\alpha \sim 50°$, flattens again and then falls steeply for pitch angles $\alpha < 10°$. This is in agreement with the suggested form of the angular distribution by Blake et al. (1980). Examples of the proton distributions are shown in Figure 6b. The proton distributions show the effect of magnetic shell splitting and, possibly, outward radial diffusion.

SC3 High Energy Particle Spectrometer

The SC3 experiment measures the energetic electron and proton distributions with good energy and angular resolution (three degree full-width-at-half-maximum). The instrument is a solid-state particle spectrometer consisting of four detector elements. Various logic combinations of the four sensors in the instrument are used to determine the particle types and energy ranges (ref. Table 3). The various particles and energy ranges are measured in time-multiplexed modes which are command-selectable. The energy spectra are obtained with a 12-channel PHA which is programmed by command.

The primary emphasis is on the electron measurements in the 47 to 4970 keV range (Reagan et al., 1981). Figure 7 shows the response of the electron fluxes to a substorm (bottom panel). The substorm injection occurred after the satellite entered the eclipse. The resultant charging of a Kapton sample on the SC1 surface potential monitor is shown in the top panel. Examples of the electron and proton spectra plus a detailed description of the experiment can be found in (Reagan et al., 1980; 1981).

SC4 Electron and Ion Beam Emission Systems

The SC4 experiment, the particle beam emission system, was to provide current sources for charging and discharging the satellite (Stevens and Vampola, 1978; Cohen et al., 1981). The electron beam emitter is basically a power triode consisting of an indirectly heated oxide-cathode, a control grid, a focusing assembly, and an exit anode at satellite ground. The range of performance parameters are shown in Table 2 and in the Stevens and Vampola (1978) report.

The ion emission system uses a cathode discharge to ionize Xenon gas which is then accelerated by a 1 kV or 2 kV potential between the ion source and the exit aperture which is at satellite ground potential. At the exit aperture there are filaments which can be heated to pro-

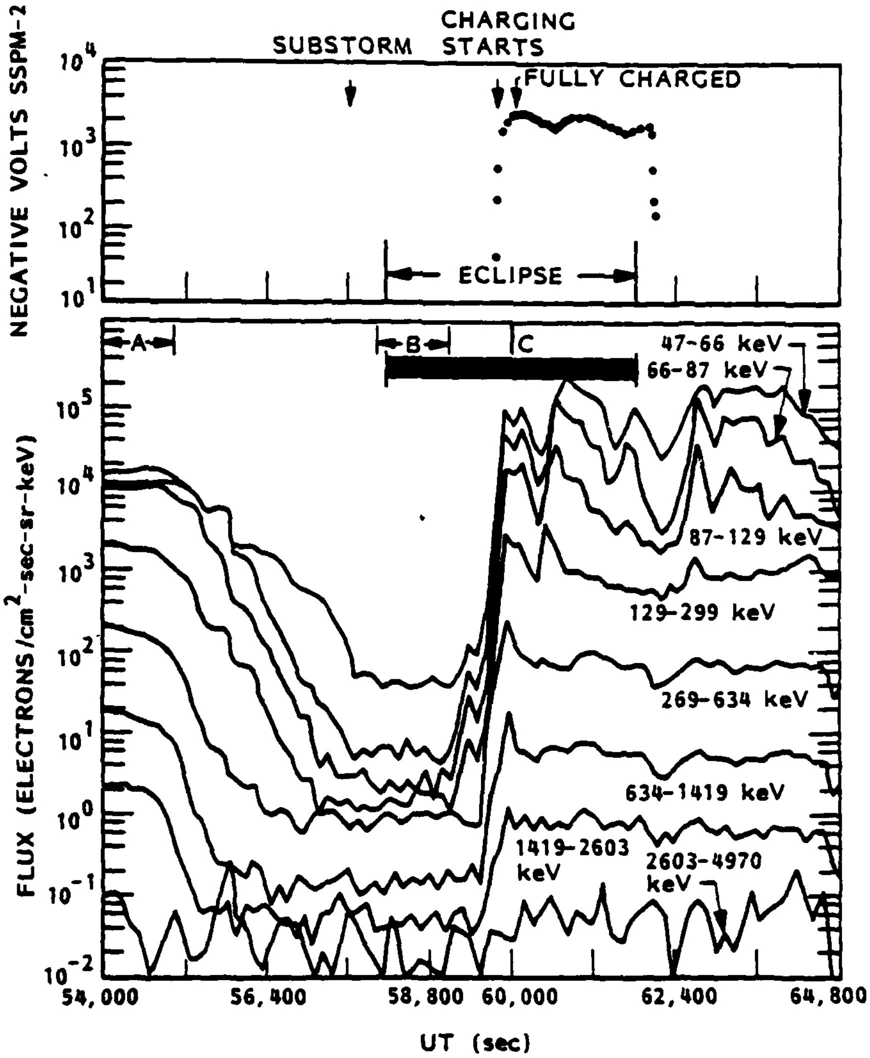

UT	15.00	15.67	16.33	16.67	17.33	18.00
LT	21.90	22.74	23.52	23.89	0.59	1.25
MLT	21.79	22.65	23.46	23.85	0.58	1.26
GLON	104.80	107.35	109.07	109.62	110.16	110.00
GLAT	-7.07	-7.61	-7.78	-7.75	-7.50	-7.03
MLAT	-18.30	-18.87	-19.05	-19.02	-18.76	-18.30
B/BO	2.09	2.21	2.23	2.23	2.27	2.34
L	6.63	6.90	7.14	7.26	7.51	7.76

Fig. 7. Top Panel. Charging voltage characteristics of a SSPM Kapton sample during eclipse on 28 March 1979. Bottom Panel. The energetic electron environment prior to, during, and after the eclipse and charging event as measured with the Lockheed SC3 experiment (after Reagan et al., 1981).

duce electrons and which can be biased. These electrons neutralize the ion beam or can be used alone as a very low energy electron source. For more details see reports by Stevens and Vampola (1978) and Cohen et al. (1981).

An example of satellite charging by the ion beam system is shown in Figure 8. The ion system is emitting a beam of 2 keV ions at various current levels. The SC2-1 spherical probe is "clamped" to within a few volts of the plasma potential by photocurrent from its surface. Thus, the probe voltage relative to the satellite represents the negative of the satellite potential. The sudden increases of satellite potential in association with the rapid decreases of ion emission current are thought to be the result of potential barrier formation at high currents which disappear at low currents (Lai et al., 1979). The details of the sheath mechanisms involved are not yet understood.

It was also determined that the neutralized ion beam emissions did stimulate plasma waves (Koons and Cohen, 1981) with the most intense emissions below the local electron gyrofrequency, typically 0.3 to 0.9 the gyrofrequency. The emissions associated with the electron beam emissions were found to change significantly when the beam current and energy were changed. Generally the wave spectrum is organized by the local electron gyrofrequency.

SC5 High Time Resolution Particle Measurements

The SC5 experiment provides electron and ion measurements over a wide range of energies (ref. Tables 2 and 3 plus Hardy et al., 1979; Stevens and Vampola, 1978) both perpendicular and parallel to the P78-2 spin axis. The energy bands of the channels are relatively wide (ref. Table 3). The electrostatic analyzer geometric factors are large as are those of the solid state telescopes. This experiment provides good counting statistics in a short sample period and thus good angular, spatial, and temporal resolution. An example of the analyzer ion data is shown in Figure 9 (top panel) for a period when field aligned ion beams were present. The corresponding SC2 data with lower temporal resolution is shown in the bottom panels. The SC5 provides a good view of the total plasma distribution in ~ 30 sec (one half spin period).

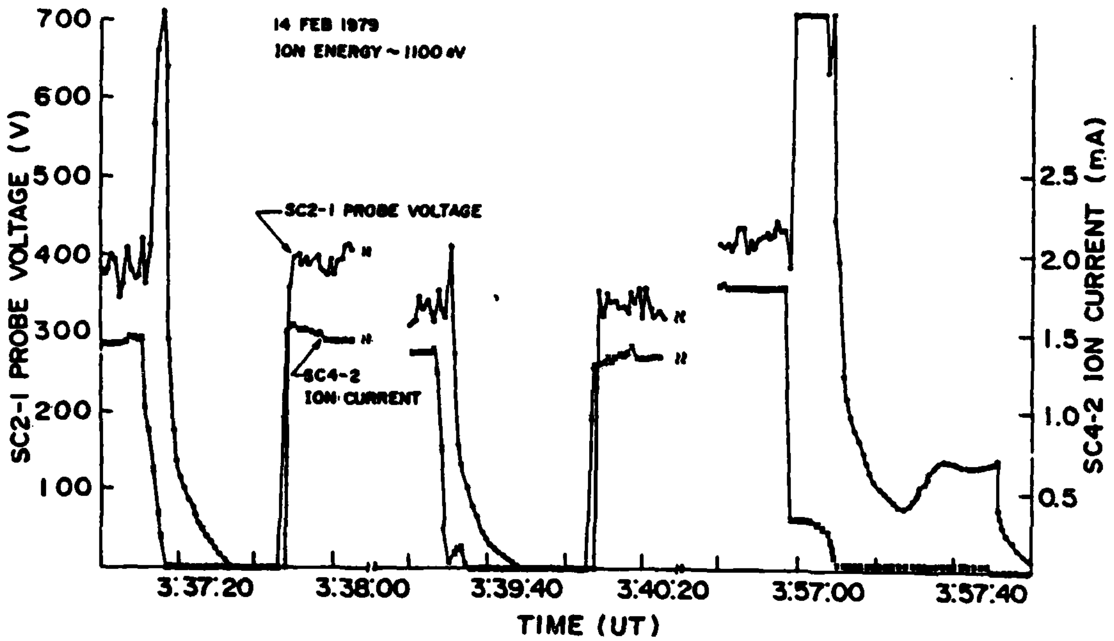

Fig. 8. SC2 probe voltage (dot points) and SC4 ion beam current (x points) taken on 14 February 1979 (after Cohen et al., 1981)

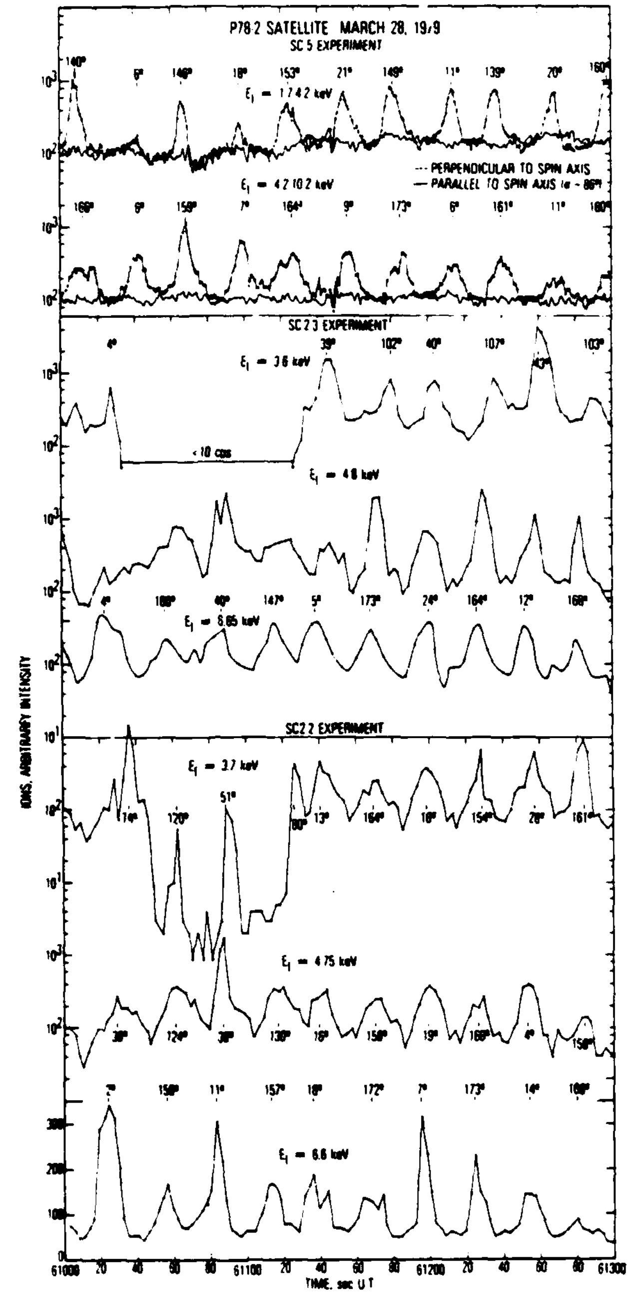

Fig. 9. Top Panel. SC5 ion intensity parallel and perpendicular to the spin axis as a function of time. Middle Panel. SC2 ion intensity perpendicular to the spin axis from the sensor mounted on the satellite body. Bottom Panel. SC2 ion intensity perpendicular to the spin axis from a boom mounted sensor, 3 m from satellite, viewing radially outward from the satellite. The pitch angles corresponding to the ion peaks are shown (after Fennell et al., 1981).

SC6 Thermal Plasma Analyzer

The SC6 instrument failed during checkout and will not be discussed further.

SC7 Light Ion Mass Spectrometer

The SC7 instrument is a combination retarding potential analyzer and ion mass spectrometer (Stevens and Vampola, 1978; Reasoner et al., 1979) which measures the density, temperature, and composition of the low-energy ions. There are three heads, one each viewing parallel and antiparallel to the spin axis and one viewing perpendicular to the spin axis (see Fig. 10). The particle energies are measured in 32 logarithmically spaced steps from 0.0 to 100 eV. The mass analyzer is sensitive to H^+, $^4He^+$, and $^{16}O^+$. The combined sensors can measure plasma flow. Figure 10 (middle) is an example of the data from the three sensors in the hydrogen mode on 12 February 1979. The data show a plasma flow as indicated at the top of Figure 10. The bottom of the figure shows a change in plasma composition from pre-flow (0400 UT) to post-flow (0426 UT). The flow apparently convected a plasma boundary past the satellite. It appears the satellite transitioned from plasmasphere to plasma sheet with a resultant decrease in the He^+/H^+ ratio (D. Reasoner, private communication, 1981). Unfortunately the SC7 experiment failed after only ten days of operation so only limited results are available.

SC8 Energetic Ion Composition Experiment

The SC8 experiment is composed of an energetic ion composition sensor measuring 100 eV to 32 keV ions and four broad-energy electron channels. The ion sensor is an ion mass spectrometer of the type flown on the S3-3 satellite (Sharp et al., 1977) with an expanded energy range. The unit measures a 32 point M/q spectrum over one of two selectable mass ranges; from 0.8 to 80 AMU and 12 to > 180 AMU. The lower mass range is the usual one. Figure 11 is an example of the ion composition measured during a magnetic storm from Johnson (1980). The data show that the O^+ density was enhanced and dominant, the H^+ density did not change much over most of the period. The energy density of O^+ is dominant for several hours at the peaks of the storms and is comparable to or larger than the H^+ energy density even at 32 keV near the storm peaks. These features

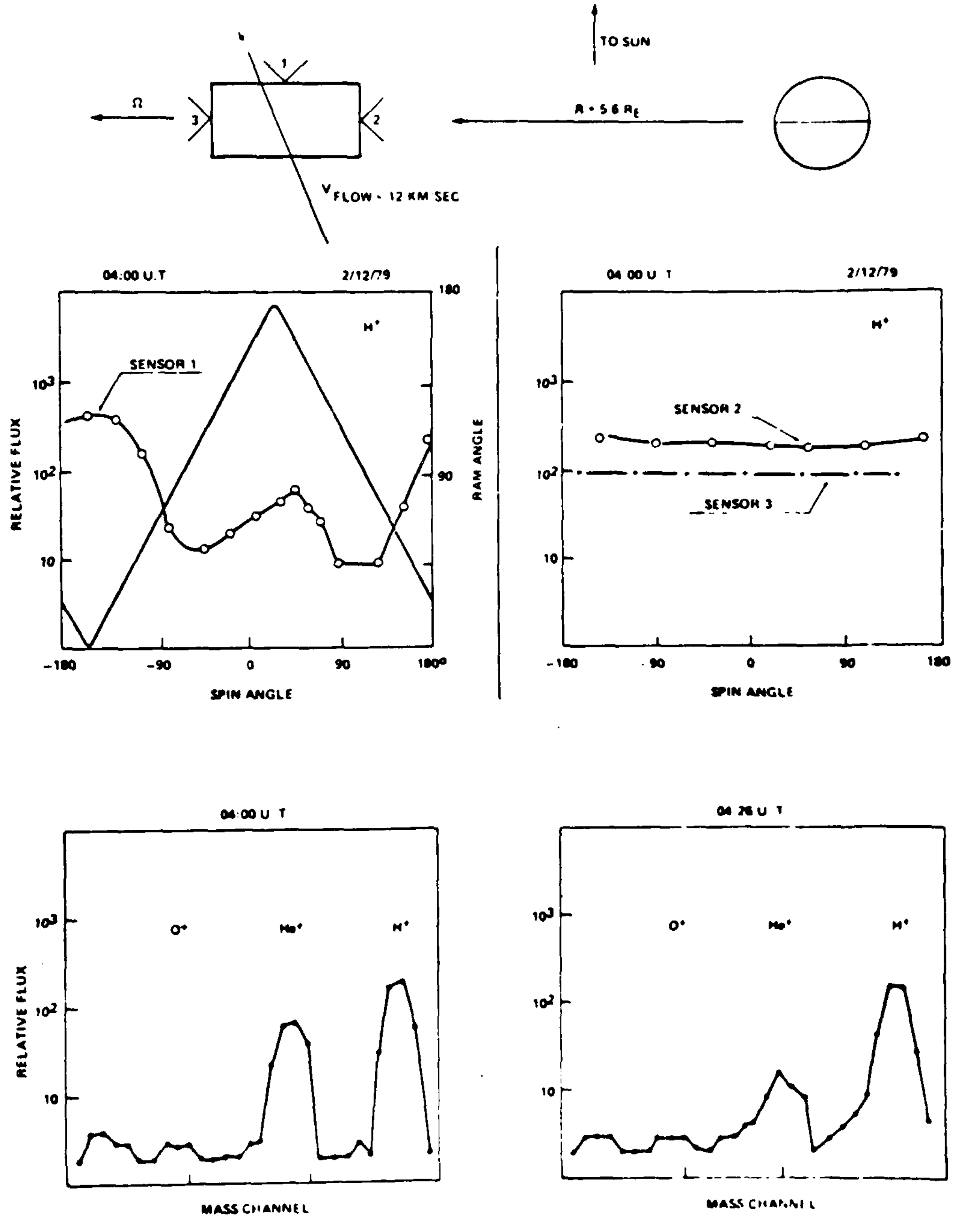

Fig. 10. Low energy ions observed by the MSFC sensor SC7 on 12 February 1979 (lower panels) and the satellite-earth geometry for these data (top panel), (from D. Reasoner unpublished data)

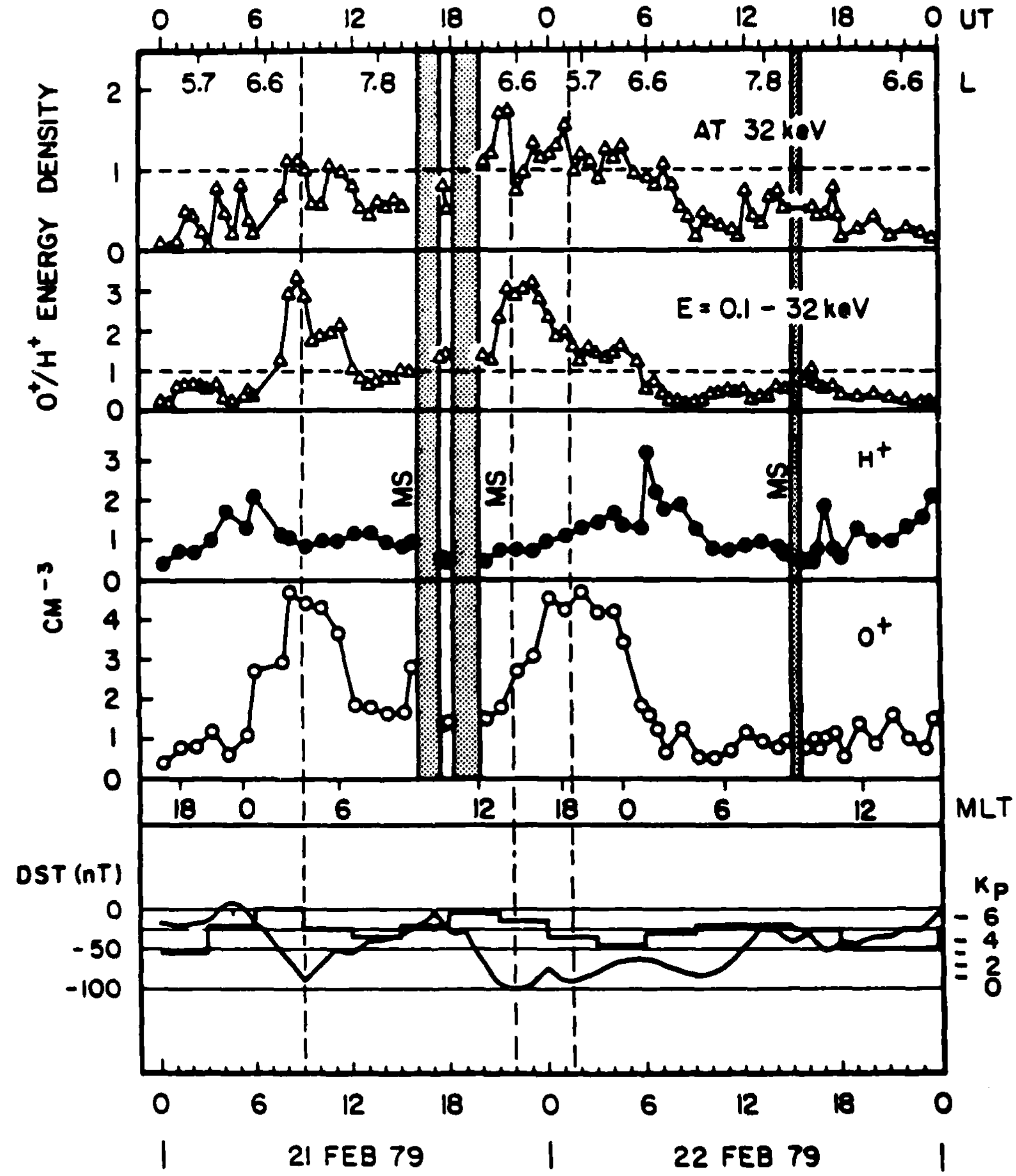

Fig. 11. Oxygen and hydrogen energy density ratios (top two panels) and densities for 0.1 to 32 keV energies (center two panels) measured by the Lockheed SC8 experiment on 21/22 February 1979. The bottom panel shows the D_{st} and Kp for this period. Taken from Johnson (1981).

are typical of six storms studied so far for 1979 (R. G. Johnson, private communication, 1981).

SC9 UCSD Charged Particle Experiment

The SC9 plasma analyzer is very similar to the one flown on ATS-6 (Olsen, 1981; Mauk and McIlwain, 1975). The instrument consists of five electrostatic analyzers, three for ions and two for electrons. Pairs of ion and electron analyzers are in rotating heads. One head is for low energies the other for higher energies (see Table 3). The third ion analyzer is a low energy unit mounted to view perpendicular to the spin axis. The rotating heads can rotate the analyzer fields of view over a range of angles (~ 220°) which includes both parallel and perpendicular to the spin axis. The two rotating heads scan in orthogonal planes.

The geometric factors are shown in Table 3 (see also Stevens and Vampola, 1978). This instrument provides the detailed plasma distribution function measurements over a reasonable period (16 sec for a spectrum), which is longer (~ 314 sec) if all pitch angles are to be covered. The sensor can also select any of the five outputs for connection via a filter to a broadband transmitter. This allows special operations in which rapid fluctuations in the particle fluxes can be followed.

Figure 12a shows sample ion distribution functions for 1 eV to 1800 eV ions. The curves show the ions are highly peaked in pitch angle near $\alpha = 90°$ for energies between ~ 10 eV to 600 eV. Figure 12b (upper curves) show that the ions are also highly peaked near the magnetic equator ($\lambda \sim 0°$). This is representative of a plasma reservoir constrained to the magnetic equator in the trough or bulge region of the plasmasphere (Wrenn et al., 1979; Olsen, 1980; Olsen, 1981). These two figures show the energy and temporal resolution of the data.

SC10 Electric Field Detector

The SC10 experiment measures the DC electric field and the satellite potential. The sensor is a 100 m tip-to-tip (50 m per side) cylindrical (0.64 cm diameter) dipole that is used as a double floating probe. The two halves of the antenna are extended perpendicular to the spin axis. The inner 30 m of each 50 m segment is coated with Kapton insulation. The digitized waveform, data filter channel and broadband out-

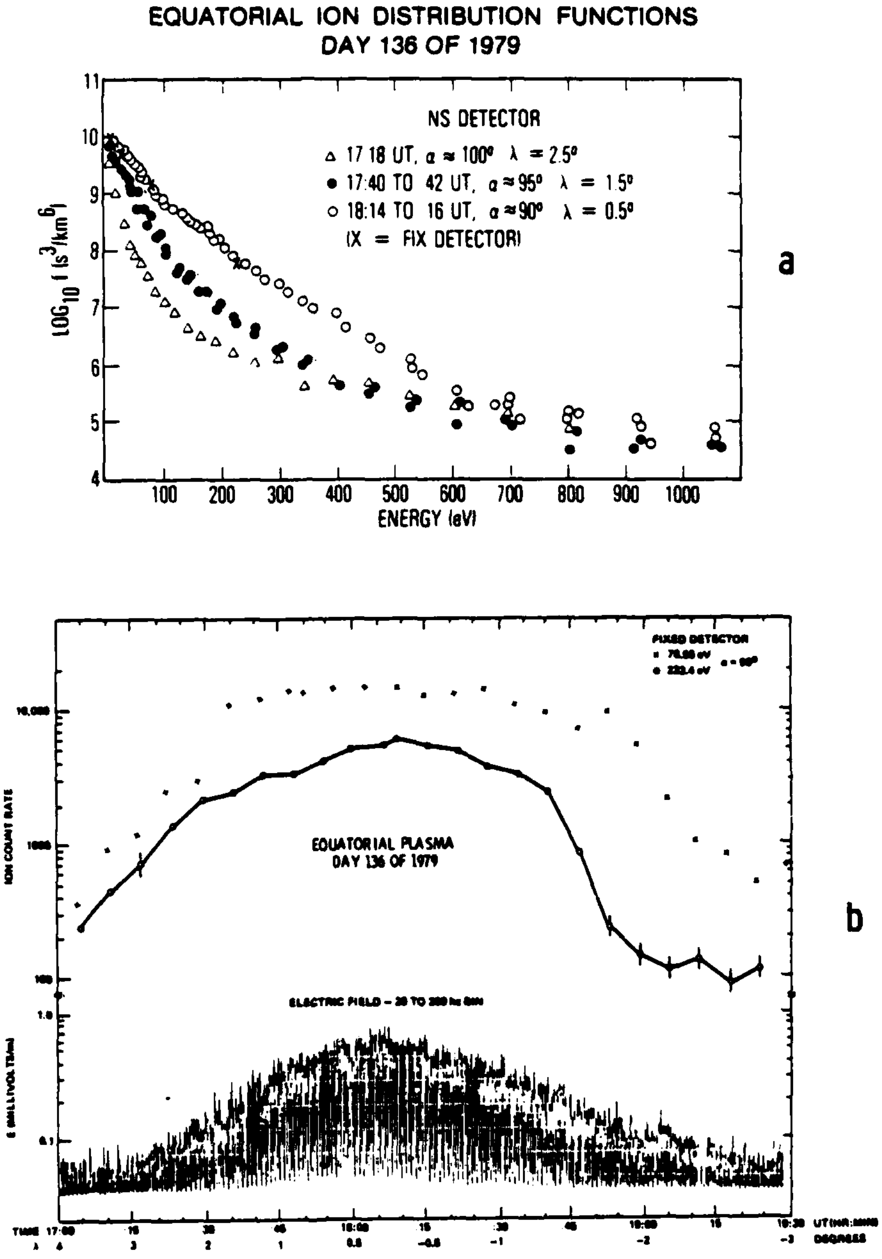

Fig. 12. (a) Ion distribution functions for selected pitch angles and magnetic latitudes taken by the UCSD SC9 experiment on 16 May 1979. (b) The ion intensity and wave intensity profiles in magnetic latitude and time on 16 May 1979. The wave data is from the GSFC electric field experiment. Taken from Olsen (1981).

puts are summarized in Table 4. The primary emphasis of the experiment is on electric fields from DC to 200 Hz. The antenna is also used by SC1 in the HF and VLF experiments.

The bottom panel of Figure 12b shows an output from the 2 to 200 Hz filter channel. This shows that low frequency waves are confined to the equator, like the plasma ions, in this case.

SC11 Magnetometer

The SC11 experiment is a triaxial fluxgate magnetometer. Each axis has a range of 0 to ± 500 nT. The sensor is mounted on a 4 m boom extended perpendicular to the spin axis. A stringent magnetics control and testing program was used to ensure an absolute accuracy of the measurements of 1 nT at one sigma confidence level on the worst axis (Stevens and Vampola, 1978). The field vector is measured four times per second. The output from the spin axis aligned sensor is also fed to a set of SC10 filter channels to provide the same frequency band (Ref. Table 4) outputs. The bandwidth of this magnetometer output is ~ 100 Hz. The same axis can be placed on a broadband channel. The filter output from SC10 provides a sensitivity of 10^{-1} nT in the 20 to 200 Hz channel while the broadband output provides a sensitivity of 0.2 nT/V.

Figure 13 shows a plot of the magnetometer data taken during a global Pc 5 event on 13 November 1979 (Higbie et al., 1981). The data is relatively clean and as shown here this event was a nice long pulsation. This pulsation is now being analyzed by several groups.

ML12 Spacecraft Contamination Experiment

The ML12 experiment provides engineering data on spacecraft contamination and changes in thermal control materials. The contamination data is provided by a quartz crystal microbalance to measure mass deposition rates. The thermal material data is provided by measuring the temperature of thermal control paint and material samples mounted on 'super' insulation. For more information on this experiment the reader is referred to the discussion in Stevens and Vampola (1978).

Transient Pulse Monitor (TPM) Experiment

Finally, the TPM is an engineering experiment

Table 4. SC10 Measurement Modes

Format	Common Mode		Differential	
digitized waveform	3 ranges	a) ±15 V b) ±300 V c) ±5,000 V	3 gains	a) X.025 b) X.25 c) X2.5
digitized fourier analyzed wave	4 frequency bands	a) 0.1 to 1.0 Hz b) 1 to 2 Hz c) 2 to 20 Hz d) 20 to 200 Hz	4 frequency bands	a) 0.1 to 1.0 Hz b) 1 to 2 Hz c) 2 to 20 Hz d) 20 to 200 Hz
FM-FM	not available		DC to 200 Hz VCO transmission up to 3 hr/day	

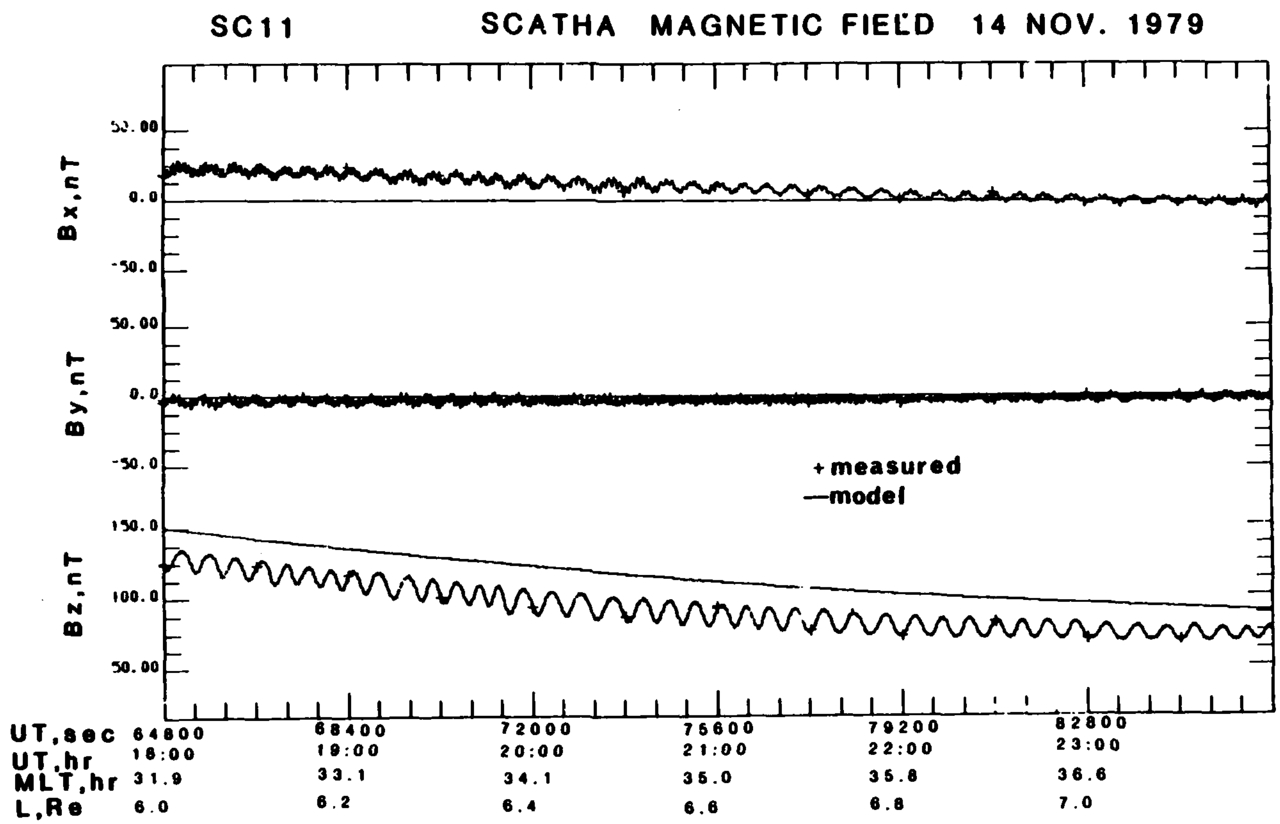

Fig. 13. Components of the magnetic field taken during a PC5 event on 14 November 1979. The model field values are from the Olson and Pfitzer (1974) model. B_z is taken in the direction of model field. B_x is in the plane defined by B_z and the radius vector from the earth to the satellite. B_y is azimuthal, completing the triad.

which provides data on the electromagnetic pulse environment on the satellite. The unit has four sensors which are built into the wiring harness. Two sensors are current probes which measure current fluctuations in the solar array power line and in the ground line of the main power system. The other two sensors are long wires mounted outside the shields of the main cable bundles. The processing electronics had commandable sensitivities. For more details see Stevens and Vampola (1978).

Summary

The P78-2 (SCATHA) satellite was placed in an orbit which extends from near the plasmasphere out to auroral magnetic field lines. This includes the inner edge of the plasmasheet. It is in perfect position to see substorm and magnetic storm effects. The placement of the spin axis in the orbit plane allows the particle experiments to obtain very good two dimensional distribution functions. The inclusion of spin axis aligned and rotating sensors helps to fill in other aspects of the complete distribution function. The use of tape recorders guarantees nearly 100% coverage and the ability to provide broadband data increases temporal and frequency resolution of both particle and wave data.

The above features are complemented by a very complete set of sensors covering a wide range of particle and field parameters. This satellite has already brought new results important to our understanding of the outer magnetosphere.

At this time about one year of data (5 February, 1979 to 17 March, 1980) have been digitized and distributed to the experimenters. Plans exist to provide digital tapes for about 50 more selected days in 1980 and 1981.

The satellite is operating perfectly as of March 1981. The original set of systems is being used. Redundant satellite systems were provided. Expendables for about a year of normal operations remain. When the expendables are near exhaustion the satellite will be shut down or reoriented with the spin axis normal to the orbit plane.

The current absence of funding by the Air Force bodes ill for continued tape digitization. Partial funding of data reduction and analysis plus the orbital operations support by experimenters was provided for about 18 months after launch. No Air Force funding is presently available for further data reduction and analysis. All the analog tapes containing the data are being stored for possible use later.

Acknowledgments. I would like to thank the many people that made the P78-2 satellite a success. These include the staffs of The Aerospace Corporation and the U. S. Air Force in the Space Test Program Offices. Thanks goes also to the members of the Air Force Satellite Control F[illegible]ility team which has operated the satellite and recovered the data. Finally, thanks must go to the U. S. Air Force Eastern Space and Missile Center for their efforts in digitizing and formatting the data. This work was performed in part under USAF Contract F04701-80-C-0081 and in part under NSF Grant No. ATM80-19060.

References

Blake, J. B., J. F. Fennell and D. Hovestadt, Measurements of heavy ions in the low-altitude regions of the outer zone, J. Geophys. Res., 85, 5992, 1980.

Blake, J. B. and J. F. Fennell, Heavy ion measurements in the synchronous altitude region, Planet. Space Sci., to be published, 1981.

Boyd, G. M., P. F. Mizera and D. R. Croley, In situ measurements of differential charging of spacecraft materials, EOS Trans. Am. Geophys. Union, 60, 924, 1979.

Cohen, H. A., R. C. Adamo, T. Aggson, A. L. Chesley, D. M. Clark, S. A. Damron, D. E. Delorey, J. F. Fennell, M. S. Gussenhoven, F. A. Hauser, D. Hall, D. A. Handy, W. B. Huber, I. Katz, H. C. Koons, S. T. Lai, B. Ledley, P. F. Mizera, E. G. Mullen, J. E. Nanevicz, R. C. Olsen, A. G. Rubin, G. W. Schnuelle, N. A. Saflekos, M. F. Tautz and E. C. Whipple, P78-2 satellite payload responses to electron beam operations on March 30, 1979, to be published in Proceedings of Spacecraft Charging Technology Conference III, N. J. Stevens, ed., Colo. Springs, Colo., 1981.

Craven, P. D. and D. L. Reasoner, Studies of mass composition and dynamics of the plasmaspheric buldge region, EOS Trans. Am. Geophys. Union, 61, 1091, 1980.

Fennell, J. F. and D. R. Croley, Jr., Preliminary results from P78-2 satellite, U. S. Air Force Space Division Report, SD-TR-81-8, 1981.

Fennell, J. F., D. R. Croley, Jr., P. F. Mizera and J. D. Richardson, Electron angular distributions during charging events, in Proceedings of Spacecraft Charging Technology Conference

III, N. J. Stevens, ed., Colorado Springs, Colo. 1981.

Hardy, D. A., W. D. Burke, M. S. Gussenhoven and J. Feynman, EOS Trans. Am. Geophys. Union, 60, 923, 1979.

Higbie, P. R., D. N. Baker, R. D. Zwickl, R. D. Belian, J. R. Asbridge, J. F. Fennell, B. Wilken and C. W. Arthur, The global Pc5 event of November 14-15, 1979, J. Geophys. Res., to be published, 1981.

Lai, S. T., W. J. Burke and H. A. Cohen, A theoretical investigation of virtual electrode formation near the SCATHA satellite, EOS Trans. Am. Geophys. Union, 60, 923, 1979.

Johnson, R. G., A review of the hot plasma composition near geosynchronous altitude, in Proceedings of the Spacecraft Charging Technology Conference III, N. J. Stevens, ed., Colorado Springs, Colo., 1980.

Koons, H. C., Characteristics of electrical discharges on the P78-2 satellite (SCATHA), presented AIAA 8th Aerospace Sciences Meeting, Pasadena, Calif., January, 1980.

Koons, H. C., P. F. Mizera, J. F. Fennell and D. F. Hall, Spacecraft charging - results from the SCATHA satellite, Astronautics and Astronautics, 18, 44, 1980.

Koons, H. C., The role of hiss in magnetospheric chorus emissions, J. Geophys. Res., in press, 1981.

Koons, H. C., Aspect dependence and frequency spectrum of electrical discharges on the P78-2 (SCATHA) satellite, in Proceedings of the Spacecraft Charging Technology Conference, N. J. Stevens, ed., to be published by NASA, 1981.

Koons, H. C. and H. A. Cohen, Plasma waves and electrical discharges stimulated by beam operations on a high altitude satellite, presented at NATO Adv. Res. Institute on Artificial Particle Beams Utilized in Space Plasma Studies, Geilo, Norway, 1981.

Mizera, P. F., H. C. Koons, E. R. Schnauss, D. R. Croley, Jr., H. K. Alan Kan, M. S. Leung, N. John Stevens, F. Berkopec, J. Staskus, W. L. Lehn and J. E. Nanewicz, Appl. Phys. Lett., 37, 276, 1980.

Mizera, P. F., SSPM charging results, J. Spacecraft and Rockets, accepted for publication, 1980.

Mauk, B. and C. E. McIlwain, ATS-6 UCSD auroral particles experiment, IEEE Transactions on Aerospace and Electronic Systems, AES-11, 1125, 1955.

Olsen, R. C., Thermal ions trapped at the equator, EOS Trans. Am. Geophys. Union, 61, 1091, 1980.

Olsen, R. C., Equatorially trapped plasma populations, unpublished manuscript, 1981.

Reasoner, D. L., P. D. Craven and C. R. Chappell, Observations of spacecraft-plasma interactions near synchronous orbit, EOS Trans. Am. Geophys. Union, 60, 923, 1979.

Reagan, J. B., R. W. Nightingale, E. E. Gaines, W. L. Imhof and E. G. Stassinopoulos, Outer zone energetic electron spectral measurements, Proceedings of the AIAA 18th Aerospace Sciences Meeting, paper AIAA-80-0390, Pasadena, CA, 1980.

Reagan, J. B., R. W. Nightingale, E. E. Gaines, R. E. Meyerott and W. L. Imhof, The role of energetic particles in the charging/discharging of spacecraft dielectrics, in Proceedings of the Spacecraft Charging Technology Conference III, N. J. Stevens, ed., Colorado Springs, Colo., 1981.

Richardson, J. D., J. F. Fennell and D. R. Croley, Jr., Observations of Field-Ion and Electron Beams from SCATHA (P78-2), J. Geophys. Res., 86, 10105, 1981.

Saflekos, N. A., J. Feynman, H. B. Garrett, D. A. Hardy, E. G. Mullen, Disappearance of particles of energies > 50 keV as seen by P78-2 (SCATHA) at near geosynchronous orbit, EOS Trans. Am. Geophys. Union, 61, 1091, 1980.

Sharp, R. D., R. G. Johnson and E. G. Shelley, Observation of an ionospheric acceleration mechanism producing energetic (keV) ions primarily normal to the geomagnetic field direction, J. Geophys. Res., 82, 3324, 1977.

Stevens, J. R. and A. L. Vampola, Description of the space test program P78-2 spacecraft and payloads, Air Force Space and Missile Systems Organization (now Space Division) report SAMSO TR-78-24, 1978.

Wrenn, G. L., J. F. E. Johnson and J. J. Sojka, Stable 'pancake' distributions of low energy electrons in the plasma trough, Nature, 279, 512, 1979.

LABORATORY OPERATIONS

The Laboratory Operations of The Aerospace Corporation is conducting experimental and theoretical investigations necessary for the evaluation and application of scientific advances to new military space systems. Versatility and flexibility have been developed to a high degree by the laboratory personnel in dealing with the many problems encountered in the nation's rapidly developing space systems. Expertise in the latest scientific developments is vital to the accomplishment of tasks related to these problems. The laboratories that contribute to this research are:

Aerophysics Laboratory: Launch vehicle and reentry aerodynamics and heat transfer, propulsion chemistry and fluid mechanics, structural mechanics, flight dynamics; high-temperature thermomechanics, gas kinetics and radiation; research in environmental chemistry and contamination; cw and pulsed chemical laser development including chemical kinetics, spectroscopy, optical resonators and beam pointing, atmospheric propagation, laser effects and countermeasures.

Chemistry and Physics Laboratory: Atmospheric chemical reactions, atmospheric optics, light scattering, state-specific chemical reactions and radiation transport in rocket plumes, applied laser spectroscopy, laser chemistry, battery electrochemistry, space vacuum and radiation effects on materials, lubrication and surface phenomena, thermionic emission, photosensitive materials and detectors, atomic frequency standards, and bioenvironmental research and monitoring.

Electronics Research Laboratory: Microelectronics, GaAs low-noise and power devices, semiconductor lasers, electromagnetic and optical propagation phenomena, quantum electronics, laser communications, lidar, and electro-optics; communication sciences, applied electronics, semiconductor crystal and device physics, radiometric imaging; millimeter-wave and microwave technology.

Information Sciences Research Office: Program verification, program translation, performance-sensitive system design, distributed architectures for spaceborne computers, fault-tolerant computer systems, artificial intelligence, and microelectronics applications.

Materials Sciences Laboratory: Development of new materials: metal matrix composites, polymers, and new forms of carbon; component failure analysis and reliability; fracture mechanics and stress corrosion; evaluation of materials in space environment; materials performance in space transportation systems; analysis of systems vulnerability and survivability in enemy-induced environments.

Space Sciences Laboratory: Atmospheric and ionospheric physics, radiation from the atmosphere, density and composition of the upper atmosphere, aurorae and airglow; magnetospheric physics, cosmic rays, generation and propagation of plasma waves in the magnetosphere; solar physics, infrared astronomy; the effects of nuclear explosions, magnetic storms, and solar activity on the earth's atmosphere, ionosphere, and magnetosphere; the effects of optical, electromagnetic, and particulate radiations in space on space systems.

DATE
ILME
-8